Boletim da Sociedade Astronômica Brasileira, **34**, no. 1, 119-123

The unique Be system HD 92406 with two stellar and two disk eclipses

T. de Amorim[1], A. Carciofi[1], J. Labadie-Bartz[2], S. Rappaport[3], A. Rubio[1], A. da Silva[1], & COPA Colaboration

[1] Institute of Astronomy, Geophysics and Atmospheric sciences/University of São Paulo. e-mail: tajan.amorim@usp.br
[2] Homer L. Dodge Department of Physics and Astronomy, University of Oklahoma.
[3] Department of Physics, Kavli Institute for Astrophysics and Space Research, M.I.T.

Abstract. About 20% of the B-type stars rotates very rapidly. Among these are the classical Be stars, which eject material and build up gaseous circumstellar decretion disks. Some models suggest that binary interaction is the dominant evolutionary pathway to acquire near-critical rotation - namely mass and angular momentum transfer. During this phase, the remaining core of the mass donor becomes a hot stripped star and the mass gainer spins up to become the Be star. To this day only about 15 rapidly rotating Be + stripped star binaries are known. HD 92406 is the second late-type Be + stripped star, occupying a unique niche in the rapidly rotating binary population. From TESS data and NRES spectral data, we were able to determine the orbital parameters as $P = 32.1854\ d$, $i > 87 \pm 1°$, $K_1 = 14 \pm 6\ km/s$ and $K_2 = 101 \pm 3\ km/s$. HD 92406 is exceptionally valuable as there are two stellar eclipses and two disk occulations per orbit. As flux from the stripped star passes through the disk, the local disk properties are encoded in the observed spectrum. This offers the unique possibility of probing the disk conditions with exquisite details. We developed a new ray-tracing code that allows the radiative transfer to be solved including the two stars as light sources and the two disks as absorbing media. Using this routine we estimated that HD 92406 is composed of a $4.45 \pm 0.16\ M_\odot$ primary Be star with temperature ranging from 12 kK (equator) to 18 kK (pole) and polar radius of $\approx 3.5\ R_\odot$, confirming it as a late type Be star. The parameters of the secondary remains still to be better constrained, but it is confirmed as a $0.62 \pm 0.29\ M_\odot$ hot subdwarf with temperatures around 20 – 30 kK and radius $R < 0.7\ R_\odot$ with strong absorption in helium lines.

Resumo. Cerca de 20% das estrelas do tipo B apresentam alta rotação. Entre elas estão as estrelas Be clássicas, que ejetam matéria e constroem discos gasosos circunstelares de 'decreção'. Alguns modelos sugerem que a interação binária é o caminho evolutivo dominante para adquirir rotação quase crítica, por meio de transferência de massa e momento angular. Durante essa fase, a estrela doadora perde suas camadas externas se tornando apenas um núcleo quente exposto e a estrela ganhadora de massa aumenta sua taxa de rotação tornando-se uma estrela Be. Até hoje, apenas cerca de 15 binárias Be + núcleo estrelar são conhecidas. HD 92406 é a segunda estrela Be de tipo tardio + núcleo estrelar, ocupando uma região única na população de Be binária. A partir dos dados do TESS e dos dados espectrais do NRES, fomos capazes de determinar os parâmetros orbitais como $P = 32,1854\ d$, $i > 87 \pm 1°$, $K_1 = 14\ pm6\ km/s$ e $K_2 = 101 \pm 3\ km/s$. HD 92406 é excepcionalmente valiosa, pois há dois eclipses estelares e duas oculações de disco por órbita. À medida que o fluxo do núcleo estelar passa pelo disco da Be, as propriedades do disco local são codificadas no espectro observado. Isso oferece a possibilidade única de sondar as condições do disco com detalhes. Desenvolvemos um novo código de rastreamento de raios que permite resolver a transferência radiativa incluindo as duas estrelas como fontes de luz e os dois discos como meios absorvedores. Usando esta rotina, estimamos que HD 92406 é composta por uma estrela Be primária de $4,45 \pm 0,16\ M_\odot$ com temperatura variando de 12 kK (equador) a 18 kK (polo) e raio polar de $\approx 3.5\ R_\odot$, confirmando-a como uma estrela Be de tipo tardio. Os parâmetros da secundária ainda precisam ser melhor restringidos, mas é confirmada como uma sub-anã quente de $0,62 \pm 0,29\ M_\odot$ com temperaturas em torno de 20 – 30 kK e raio $R < 0,7\ R_\odot$ com forte absorção nas linhas de hélio.

Keywords. emission-line, Be – binaries: eclipsing

1. Introduction

As discussed in Georgy et al. (2013), high rotational speeds can significantly alter the evolution of a massive star. One effect of rotation is the increased chemical mixing in the stellar interior, whereby the core (metals) and envelope (namely hydrogen) exchange materials, thus rejuvenating the core in hydrogen and extending the main sequence lifetime. Rapid rotation has additional consequences, such that the star becomes oblate (being up to 1.5 times larger at the equator compared to the pole) and strong gradients in temperature and surface gravity develop (being cooler and presenting lower surface gravity at the equator). However, despite the major role that rotation plays in stellar structure and evolution, the details remain poorly understood.

The so-called Be stars (= B stars with Balmer emission lines) display the most extreme consequences of rotation, having near-critical rotation rates which allows them to build up a circumstellar decretion disk. These gaseous circumstellar disks are built from the mechanical ejection of mass and angular momentum from the stellar surface. These properties of Be/Oe stars make them excellent laboratories to study the behavior and interplay of stellar winds, pulsation, interior processes and other phenomena in fast rotators (Rivinius, Carciofi & Martayan 2013). Most relevant here is that the angular momentum (AM) content of the disk entirely comes from the central Be star. Thus, by characterizing the disk, we learn about the flux of AM out of the star, which has significant implications for stellar evolution (Granada et al. 2013).

It has been suggested that spin-up through binary interaction can explain most, if not all, of the rapidly rotating OB population (Kriz & Harmanec 1975; Pols et al. 1991; Hastings et al. 2021). However, since the (surviving) remnant of the initial mass-donor is often very small, they are generally difficult to detect, and thus the binary incidence of the rapidly-rotating OB population remain poorly constrained. On the other hand, there are also predictions that single-star evolution can produce the majority of the present-day rapid-rotators (Martayan et al. 2006; Georgy et al. 2013). The solution to this conflict between single-star versus binary evolution requires observations suitable for the discovery and classification of relatively small stellar remnants (or to rule them out), as well as characterizing

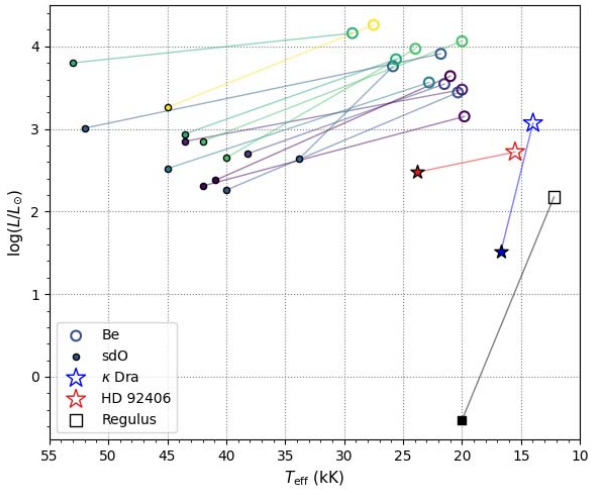

Figure 1. The luminosity and $T_{\rm eff}$ for most of the known Be+sdO binaries and for HD 92406 . In each system, the B star is plotted as an open circle/star, and the sdO star as a filled circle/star, with dashed lines connecting the two components of a given system. Colors correspond to the B star mass (lighter for more massive Be stars). The Regulus system, made up of a rapidly-rotating B8V star and a 'pre-WD' are shown as squares. HD 92406 occupies a unique location in this diagram, somewhat intermediate between the early-type Be+sdO binaries and the less massive Regulus system, similar to κ Draconis (shown as blue stars), the only other late type Be+sdB known.

other consequences of binary interaction (*e.g.* run-away stars after disruption from a supernova, abundance patterns indicative of mass transfer and/or mergers).

There are ∼15 known binaries where the primary (the optically brighter star) is an early-type rapidly-rotating classical Be star and the secondary is a hot stripped star (typically a hot subdwarf, sdOB, Wang et al. 2021). Fig. 1 shows the luminosity and temperature for both components of most known Be+sdO binaries. Their evolutionary path is one in which the initially more massive star evolved and initiated mass transfer via Roche lobe overflow. While the details of such interactions are an active field of research, the end result is that the mass-gainer acquired mass and angular momentum (thus achieving a high rotation rate), and the exposed core of the mass-donor remained as a hot stripped star (hereafter referred to as an sdO for convenience). Thus, the observed Be+sdO stars are in an evolutionary stage after binary mass transfer, but before the rapid rotator has evolved (far) from the main sequence (and before any SNe; Van Bever & Vanbeveren (1997); Shao & Li (2014)).

The Be X-ray binaries (BeXRBs) are a higher-mass more-evolved analog of the Be+sdOB binaries where the companion is a neutron star (NS), having previously exploded as a supernova (Rappaport & van den Heuvel 1982). To date, only two examples of a lower-mass analog has been discovered – the Regulus system contains a rapidly-rotating B8 star and a 'pre-white dwarf' companion (Gies et al. 2020; Rappaport, Podsiadlowski & Horev 2009) – the κ Draconis system contains a B6e and a sdB companion (Klement et al. 2022).

In Be+sd0 systems, the characterization of the subdwarf is almost always a tough challenge. This is due to the low luminosity of the companion making it impossible to differentiate using only spectra. κ Draconis is an example where the companion orbital characteristics were obtained astrometrically. This is further complicated by the fact that small angular separations are better resolved in IR, where the companion is much more weaker than the Be. In this scenario, HD 92406 is one of a kind.

HD 92406 is a 32 d Be binary initially described as two similar stars by Hauck (2018). Here we suggested it to be the second putative late-type Be+sdOB binary, which not only occupies a unique niche in the rapidly rotating binary population, but also has a favorable contrast ratio in the visible such that the features of the hot small companion are readily detectable given our preliminary modelling of the system with the available optical data. With its two stellar eclipses, and two broad disk eclipses, this is a uniquely valuable system for studying the origin of rapid rotation in hot stars, binary stellar evolution, and disk physics.

2. Differential photometry

2.1. TESS - Light Curve

The Transiting Exoplanet Survey Satellite (TESS, Ricker et al. 2015) has observed the photometric variability of HD 92406 in 3 sectors: sector 10 in 2019 and sector 36 and 37 in 2021. The overall shape of the TESS light curve (Fig. 2) reveals two short and deep eclipses (the normal stellar eclipses) and two broad and shallow eclipses. The proposed explanation is that the Be star present a standard viscous decretion disk (Rivinius, Carciofi & Martayan 2013) structure truncated by the companion, while the sdOB present a small accretion disk with asymmetries due to tidal forces. In Fig. 3 we present a SPH simulation (Smooth Particle Hydrodynamics) for a system with stellar, disk, and binary properties similar to those of HD 92406 (Rubio et al., in prep.). In brief, the gravitational influence of the companion star causes quasi-permanent structure in the Be disk, phase locked to the binary orbit, manifesting as a pair of (unequal) spiral arms where the local density is enhanced (Panoglou et al. 2018; cyr et al. 2020; Peters et al. 2008). The spiral arms are probably the main reason for the asymmetries in the primary disk eclipse. All the structures appear to be fairly stable in a 2 years basis, although small changes in the depth of the disk eclipses may indicate a slow dissipation of both disks.

Normally, we would be able to obtain the stellar radii by a simple geometric solution of the eclipse of 2 spheres. In this case, however, the oblate shape of the Be star, usually described by the critical velocity parameter (W) (Rivinius, Carciofi & Martayan 2013), adds a definite complication layer. W not only affects the eclipse shape, it may also affect the eclipse duration in a complicated way and disallow the assumption of an isothermal photosphere because of the gravity darkening effect. Therefore, the radii determination needs sophisticated models, which was achieved in Section 4.

2.2. COPA colaboration - CMD

The color magnitude diagram (CMD, Figure 4) was obtained in partnership with the COPA collaboration from the Brazilian Astronomical Society, which seeks to unite professional and non-professional astronomers in order to produce significant astrophysical research. Within this collaboration, we have obtained multi-color absolute photometry in the BVR Johnson bands. In the CMD, the flat portion of the light curve, where nothing is being eclipsed, is characterized by V ≈ 9.1 and B − V ≈ 0.0075. Both the primary stellar (V ≈ 9.35 and B − V ≈ 0.08) and disk (V ≈ 9.2 and B − V from 0.02 to 0.06) occultations are perceived as a clear reddening, as the hotter smaller star is being eclipsed. The corresponding signal from the CMD path of the secondary eclipse is definitely much weaker and thus harder to identify. The secondary stellar eclipse is marked by a weak shift to bluer parts

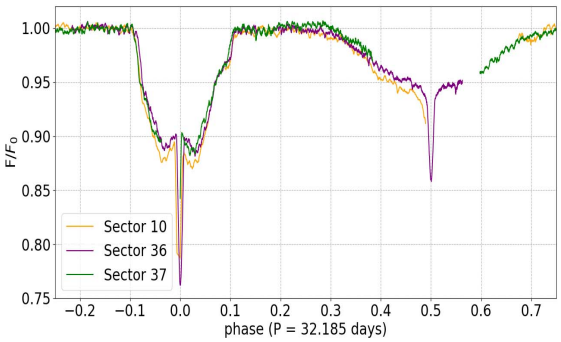

Figure 2. TESS photometry from ~3 months (sectors 10, 36, 37) phased to the orbital period (32.185 d). Features include the hotter companion star being eclipsed by the Be disk (the broad dip between Phase = -0.1 – 0.1), the stellar eclipse of the sdOB star (the deep sharp eclipse at Phase = 0), the Be disk being partially eclipsed by the companion (the broad shallow feature between Phase = 0.3 – 0.7), and the eclipse of the Be star at Phase = 0.5. Smaller-amplitude higher-frequency signals are evident, caused by non-radial pulsation of the Be star and also the companion.

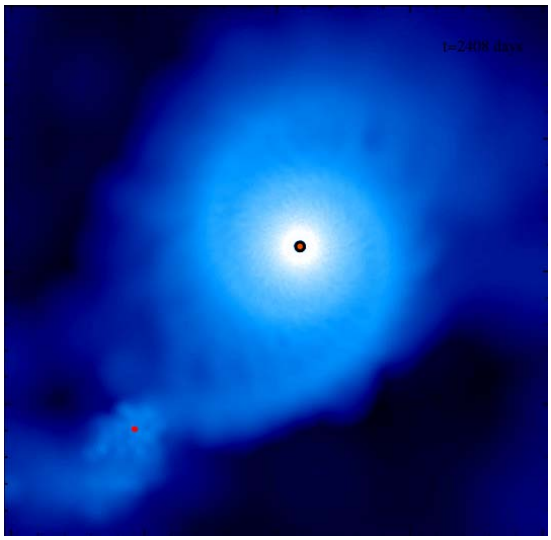

Figure 3. SPH simulation for HD 92406 considering two disks and the $m = 2$ wave generating the spiral arms. The stars, which are not in physical scale, are marked by red circles.

($V \approx 9.15$ and $B - V \approx -0.01$), as the colder star is being partially eclipsed. The secondary disk occultation presents no clear signal.

3. Orbital Solution

The Network of Robotic Echelle Spectrographs (NRES) from the Las Cumbres Observatory (LCO) provides high resolution ($R \approx 53000$) spectra in the optical range (390 - 860 nm Siverd et al. 2018). The observations consist of 30 min expositions with a 1m telescope. The system was observed 23 times with the intention to maximize the orbital coverage. The dynamical spectra (Fig. 5) indicates that some lines are clearly from the primary (*e.g*, FeII5316) while others are from the secondary (*e.g.*, HeI5875).

The Balmer emission lines, represented by the H_α, confirm the existence of a circumstellar disk around the primary star, and thus its Be status. The primary star also present strong iron lines

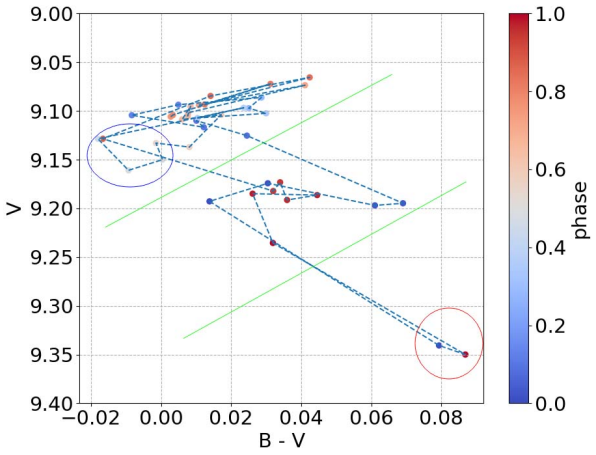

Figure 4. Color magnitude diagram for HD 92406 produced by the COPA collaboration. The open circles corresponds to the region of the stellar eclipses, where red relates to the primary eclipse and blue to the secondary eclipse. The 2 green lines limit the primary disk occultation.

Figure 5. Dynamical plots for HD 92406. The top panels present lines from the primary star/disk. The bottom panels present lines (or lack of) from the secondary star. The red line indicates the orbital velocity of the star.

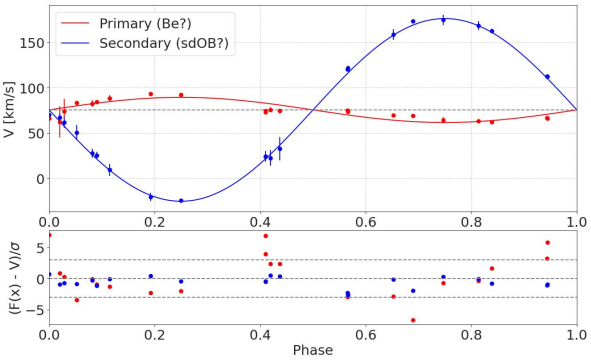

Figure 6. Radial velocity curve for both stars in HD 92406. The velocity data were obtained from line fitting of 23 NRES observations. The lines used to calculated the primary star velocity were FeII5169, FeII5316 and FeII5362. The lines for the secondary were HeI4713, HeI5875, HeI6678.

such as FeII5316. These lines display the normal shell feature expected from Be stars seen edge-on, which means that the deepest part of the lines is affected by disk absorption. The lack of any Helium absorption feature with low velocity indicates that the primary may be a late type Be. The secondary star shows clear and strong HeI lines but no signal in HeII lines. This indicates a spectral type of early B rather than an O star.

The difference in temperature of the stars enables us to determine the orbital motions, via absorption lines, with almost no contamination from the companion. For each star, the 3 most prominent lines were fitted using a simple Gaussian fitting routine. The radial velocity for each phase was considered to be the median velocity obtained in the 3 absorption lines. In Figure 6, the final velocity curve is depicted.

Table 1. Orbital parameters derived from the radial velocity curves of Fig 6. K corresponds to the orbital velocity of each star. V_g corresponds to the system radial velocity. M represents the masses of each star. The uncertainty in velocity was estimated by the Levenberg–Marquardt algorithm and the uncertainty in mass was calculated by propagation.

Parameter	Primary	Secondary
K [km/s]	14 ± 6	101 ± 3
V_g [km/s]	75 ± 1	
M [$M_\odot$]	4.45 ± 0.16	0.62 ± 0.29

Table 2. Best model achieved using a Levemberg-Marquadt algorithm. The corresponding light curve is depicted in Fig. 7. T_p and R_p defines the polar temperature and radius, respectively. W is the critical velocity parameter. n_0 is the density at the base of the disk. i is the viewing angle.

Parameter	Primary	Secondary
T_p [kK]	17.0	23.8
R_p [$R_\odot$]	2.67	1.02
W	0.83	0.06
n_0 [10^{13}cm^{-3}]	5.3	1.9
i	88°	

To obtain the orbital parameters, we used a simple Levemberg-Marquadt algorithm, the results are shown in Table 1. As the obtained eccentricity was very small, we have found that restricting the simulations to circular movement yield similar results and makes the simulation easier in both the orbital solution and all the modeling effort in Section 4. The presence of eclipses indicates that $i > 87°$, therefore we assumed $\sin(i) = 1$ for the calculations. This yields masses of 4.45 $M_\odot$ for the primary and 0.62 $M_\odot$ for the secondary. There are two main reasons for the high uncertainty in the mass of the secondary: The large mass ratio ($q = M1/M2 \approx 7.2$) which in turn dictates a scenario with low orbital velocity for the primary, thus harder to be measured and the presence of a disk, which may be responsible for subtle changes in the line shape, mainly in the eclipses.

4. Ray Tracing routine

Modelling a light curve of eclipsing binaries is generally not a huge problem as we can approximate the system by two spherical stars of uniform intensity. In HD 92406, this picture becomes much more intricate as we need to consider the effect of oblateness in the primary star as well as the presence of one or two disks. To solve this issue we have created a ray tracing routine that can compute the observed composite spectra for each orbital phase. The routine can add the spectra of each object, considering the doppler shift, limb darkening and gravity darkening, and includes both stellar eclipses and the absorption of light (attenuation) due to both disks. Figure 7 illustrates the capability of the routine.

We are currently running this routine using the Levemberg-Marquadt method to achieve the best fit. In Figure 7, we show the best model achieved until now. These values are initial estimates only, as the work is still ongoing. However, the results are encouraging, as the main features of the primary eclipse (width, depth, the rise before the stellar eclipse and latter itself) were well reproduced.

The parallax measurement contains an inconsistency for HD 92406. Gaia Data Release 3 (GDR3, Gaia Collaboration 2016, 2022) locates this system at $0.85^{+0.33}_{-0.19}$ kpc, but with a bad

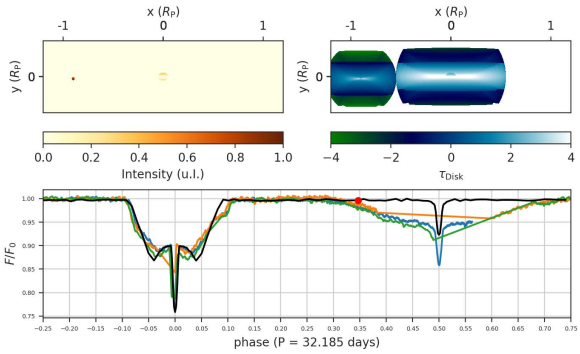

Figure 7. Simulation of HD 92406. The represented results are preliminary models that show the results of the ray-tracing code designed specifically for this project. Bottom: TESS photometry (colored lines). The modeled light curve is represented in black. The red dot corresponds to the phase represented in the upper panels. Top: Map of Intensity (left) and optical depth (right) resulting from the ray tracing routine. R_p corresponds to the primary equatorial radius.

re-normalised Unit-Weigth Error (RUWE) which is higher than 14. lindegren et al. (2018) pointed out that the criteria for good solutions should be RUWE < 1.4. In the analysis of Bailer-Jones et al. (2021), they found the geometric distance as $2.1^{+1.4}_{-1.2}$ kpc and the photogeometric distance as $0.80^{+0.20}_{-0.13}$ kpc. Because of this inconsistency in the distance measurement, we opted to consider the distance as a free parameter rather than an input.

To generate the composite spectra, we used the Hdust code (Carciofi & Bjorkman 2006, 2008), which computes the radiative transfer in gaseous and dusty media. This code is important because it can calculate the disk temperature structure for an isolated star. With the described model from Fig. 7, we used the HDUST code to obtain the spectra in Fig 8. The obtained parameters revealed to be quite consistent with the observed spectral energy distribution, showing that indeed the secondary star is still relevant for the composite spectra even in large wavelengths. The distance was fitted to be ≈ 0.86kpc, consistent with the GDR3 distance and the photogeometric distance from Bailer-Jones et al. (2021). E(B-V) was also considered as a free parameter and was estimated in E(B-V) = 0.065, consistent with the value measured by GDR3, of E(B-V) = 0.047.

5. Final Discusson

Although this work is still not complete, we show strong evidences, with spectroscopy and photometric data, that HD 92406 is indeed a system composed of a late type Be + sdB star. Further work is still needed to fully characterize both stars. Such determination is important because this system present possibilities like no other to comprehend the structure of Be + sdOB systems, not only physical information of the stars but also their disks. The goal is that the results from this work may help us in determining the evolutionary path that similar systems may undergo.

The secondary disk eclipse cannot be explained by our simulations. This is the main issue that we will be working on in the following months. Our hypothesis is that either a circumbinary disk or a asymmetric secondary disk would be able to represent the broad secondary eclipse. Both hypothesis can be tested as long as we consider a real disk hydrodynamic simulation, which will be in our path.

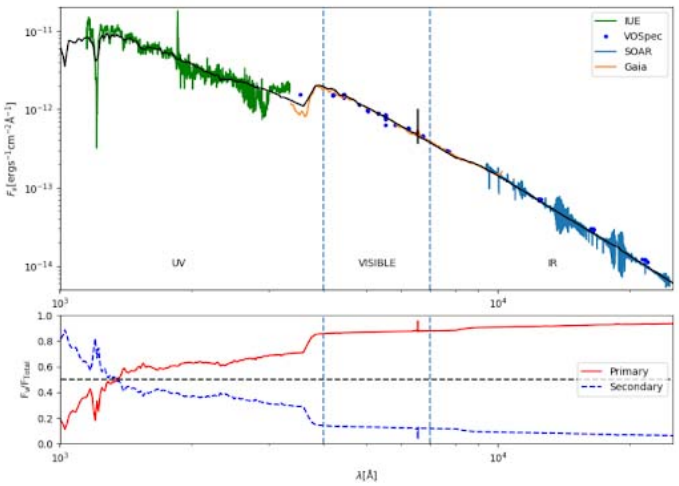

Figure 8. Top panel: Spectral energy distribution for HD 92406. The black line is the modeled spectra. The colored lines represent the observed data, blue for the International Ultraviolet Explorer, orange for Gaia DR3 Gaia Collaboration (2022) and blue for Goodman spectrograph in the Southern Astrophysical Research Telescope (SOAR, Clemens, Crain & Anderson 2004). Bottom panel: Contribution of each star for the composite spectra. The secondary dominates for very low wavelengths, but in contrast to the majority of Be + sdOB system, continues to be relevant in the visible with contribution of at least 10 %.

Acknowledgements. T.H.A. acknowledges the public research funding in Brazil which was crucial to the development of this project, in especial FAPESP (grant 2021/01891-2). A.C.C. acknowledges support from CNPq (grant 311446/2019-1) and FAPESP (grants 2018/04055-8 and 2019/13354-1). This works makes use of the public available observations from the Transiting Exoplanet Survey Satellite (TESS), the International Ultraviolet Explorer (IUE) and from the Gaia Data Release 3. This work has made use of private observations from the Southern Astrophysical Research Telescope (SOAR) and the Las Campanas Observatory (LCO). The simulations were computed using the structure of the Laboratory of Astroinformatic (LAi) from the University of São Paulo, that made this work possible.

References

Bailer-Jones, C., Rybizki, J., Fouesneau, M., Demleitner, M., Andrae, R., 2021, AJ, 161, 147
Carciofi, A., Bjorkman, J., 2006, ApJ, 639, 1081.
Carciofi, A., Bjorkman, J., 2008, ApJ, 684, 1374.
Clemens, J., Crain, J., Anderson, R., 2004, The Goodman spectrograph, Moorwood, A., Iye, M., 5492, 331-340
Cyr, I., Jones, C., Carciofi, A., Steckel, C., Tycner, C., Okazaki, A., 2020, MNRAS, 497, 3525.
Eldridge, J., Stanway, E., Xiao, L., McClelland, L., Taylor, G., Ng, M., Greis, S. and Bray, J., 2017, PASA, 34, e058.
Gaia Collaboration et al., 2016, A&A, 595, A1.
Gaia Collaboration et al., 2022, arXiv:2208.00211.
Georgy, C., Ekström, S., Eggenberger, P., et al., 2013, ApJ, 558, A103.
Gies, D., Bagnuolo Jr, W., Ferrara, E., Kaye, A., Thaller, M., Penny, L. and Peters, G., 1998, ApJ, 493, 440.
Gies, D., Lester, K., Wang, L., Couperus, A., Shepard, K., Neiner, C., Wade, G., Dunham, D. and Dunham, J., 2020, AJ, 902, 25.
Granada, A., Ekström, S., Georgy, C., Krtička, J., Owocki, S., Meynet, G., and Maeder, A., 2013, A&A, 553, A25.
Hastings, B., Langer, N., Wang, C., Schootemeijer, A., and Milone, A. P., 2021, A&A, 653, A144.
Hauck, Norbert, 2018, arXiv:1805.04318
Klement, R. et al., 2022, ApJ, 940, 86
Kriz, S. and Harmanec, P., 1975, Bull. Astron. Inst. Czechoslov., 26, 65
Lindegren, L., 2018, Gaia Technical Note: GAIA-C3-TN-LU-LL-124-01.
Martayan, C., Frémat, Y., Hubert, A. -M., Floquet, M., Zorec, J. and Neiner, C., 2006, A&A, 452, 273
Panoglou, D., Faes, D., Carciofi, A., Okazaki, A., Baade, D., Rivinius, T., Borges Fernandes, M., 2018, MNRAS, 473, 3039.
Peters, G., Gies, D., Grundstrom, E., McSwain, M., 2008, AJ, 686, 1280.
Pols, O. R., Cote, J., Waters, L. B. F. M., Heise, J., 1991, A&A, 241, 419.
Rappaport, S., Podsiadlowski, Ph. and Horev, I., AJ, 698, 666
Rappaport, S. and van den Heuvel, E., 1982, X-ray observations of Be stars, Jaschek, M. and Groth, H., 327
Ricker, G. et al, 2015, J. Astron. Telescopes, Instrum., Syst., 1, 014003.
Rivinius, T., Carciofi, A., and Martayan, C., 2013, A&A, 21, 69.
Shao, Y. and Li, X., 2014, AJ, 796, 37.
Siverd, R. et al., 2018, Ground-based and Airborne Instrumentation for Astronomy VII, Evans, C., Simard, L., Takami, H., 10702, 107026C
van Bever, J. and Vanbeveren, D., 1997, A&A, 322, 116.
Wang, L., Gies, D., Peters, G., Götberg, Y., Chojnowski, S., Lester, K. and Howell, S., 2021, AJ, 161, 248.